Novel uniplanar flexible Artificial Magnetic Conductor

M. E. de Cos[1], and F. Las Heras[1]

[1]Area de Teoría de la Señal y Comunicaciones. Dpt. Ingeniería Eléctrica, Universidad de Oviedo.
Edificio Polivalente, Mod. 8. E-33203 Gijón, Asturias, Spain
*M. E. de Cos, E-mail: medecos@tsc.uniovi.es

Abstract

A novel flexible uniplanar Artificial Magnetic Conductor (AMC) design is presented. A prototype is manufactured and characterized under flat and bent conditions in anechoic chamber. The designed prototype shows broad AMC operation bandwidth, polarization angle independency and high angular stability margin when operating under oblique incidence.

1. Introduction

Metamaterials exhibit unique properties in controlling the propagation of electromagnetic waves which make them very attractive as potential solution for some microwaves circuits and antennas problems.

At microwave frequencies, uniplanar Frequency Selective Surfaces (FSSs) over a metallic ground plane can be used as Electromagnetic Band-Gaps (EBGs) (exhibiting one or several frequency bands in which no mode propagation is allowed) or as Artificial Magnetic Conductors (AMCs) (exhibiting in-phase reflection). In the absent of via holes, both EBG frequency band and AMC frequency band do not necessarily coincide [1]. At the resonance frequency, both EBGs and AMC structures, exhibit high impedance surface and so they are also called High Impedance Surfaces (HIS) [2]-[6].

AMCs are electromagnetically dual to Perfect Electric Conductors (PEC) and behave as Perfect Magnetic Conductors (PMCs) over a certain frequency band (as PMCs do not exist in Nature), the so-called AMC frequency band. AMCs can be used as reflectors, in the design of low-profile and highly efficient antennas and to reduce the antenna radiation to the body in wearable applications.

The interest in flexible AMCs is growing since it would be desirable to have AMC being object-shape-adapted for many applications as RFID tags over metallic objects [7], wearable antennas [8]-[11] and RCS reduction [12]-[13]. This would require the AMC to be flexible but without losing its functionality. In addition, the AMC performance for different polarization of the electrical incident field (under normal incidence) and under oblique incidence is very important. AMC designs with as higher angular stability as possible are desirable [14].

In this contribution a novel flexible AMC design is presented in section 2. It has several additional advantages as being uniplanar, compact and without via holes which makes it cost-reduced. A prototype of the flexible AMC is manufactured using a bendable dielectric substrate. Section 3 describes the AMC prototype characterization process and results, showing that in addition, the novel design exhibits broad AMC operation bandwidth together with high angular stability in both flat and bent conditions. Finally, some conclusions are given in section 4.

2. AMC design

Each unit-cell of an AMC structure implements a distributed LC network with one or more resonance frequencies at $1/\left(2\pi\sqrt{LC}\right)$ where the structure exhibits high surface impedance meanwhile the in-phase reflection bandwidth is proportional to $\sqrt{L/C}$. At frequencies below the resonance frequency the surface impedance of the periodic structure is inductive and supports TM waves whereas at frequencies higher than the resonance frequency, the surface impedance is capacitive and supports TE waves.

The unit-cell geometry together with the substrate relative permittivity and thickness mainly determine the AMC resonant frequency and AMC frequency bandwidth. So those are the elements modified by a designer in order to obtain an AMC at a specific frequency and with a given bandwidth. To increase the AMC bandwidth a thicker dielectric substrate is needed, as it increases the equivalent L, meanwhile it decreases the resonance frequency. Another way of increasing the equivalent L and so the AMC bandwidth, is including narrow strips in the geometry design. In addition, by reducing the substrate's relative dielectric permittivity ε_r and increasing the gap between adjacent unit-cells the equivalent C can be reduced and the AMC bandwidth will be also increased. Finally, it has to be taken into account that higher ε_r reduces the resonance frequency and the AMC bandwidth. In sum, to obtain both compact size and broad AMC operation bandwidth a trade-off solution has to be taken considering substrate thickness and ε_r.

Taking all these facts into account a uniplanar AMC [15]-[16] at 6GHz has been designed using ROGER3003 substrate with a thickness h=0.762 mm, relative dielectric permittivity ε_r = 3.0 and loss tangent tgδ=0.0013. The geometry of the AMC unit-cell is shown in Fig. 1 and the

final optimized dimensions for operation at 6GHz using Ansoft HFSS [17] are detailed in table I.

HFSS simulation set-up used to obtain the reflection coefficient phase based on Finite Element Method (FEM) and Bloch-Floquet theory is shown in Fig.2. It models a single unit-cell of the structure with periodic boundary conditions (PBCs) on its sides, to resemble the modelling of an infinite structure [2],[15]. To illuminate the periodic surface normal plane waves are launched using a waveport positioned a half-wavelength above it. The phase reference plane is taken on the periodic surface and the phase of the reflection coefficient for the AMC structure is compared to that of a PEC plane taken as reference, placed at exactly the same position as the AMC, in the same way as in [2].

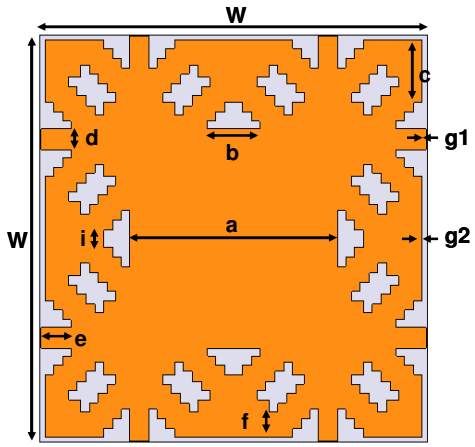

Figure 1: AMC unit-cell geometry top view.

Table 1: Unit-cell dimensions.

Dimensions (mm)				
W	**a**	**b**	**c**	**d**
12.000	6.456	1.646	1.827	0.609
e	**f**	**g1**	**g2**	**i**
0.945	0.730	0.032	0.154	0.522

Fig. 4 shows the reflection coefficient phase simulation [15] results for the designed AMC. As it could be expected, at low frequencies compared to the resonance frequency, the reflection coefficient phase is 180º, and the periodic structure behaves like a PEC. The reflection phase crosses through zero at the resonance frequency and returns to -180º above it. When the surface impedance exceeds the free space impedance the reflection phase falls in -90º, 90º. Image currents are in-phase rather than out of phase within this range, as in a PMC, and for this reason it is generally considered the AMC operation bandwidth. The inherent in-phase reflection property of AMCs makes possible antenna elements lay directly on the periodic surface without being short-circuited or malfunctioning.

From the reflection coefficient phase simulation results (see Fig.4) an AMC operation bandwidth of 500 MHz (8.33%) is obtained under normal incidence. It is a broad bandwidth for a very thin AMC (λ_0/65.6 at 6GHz).

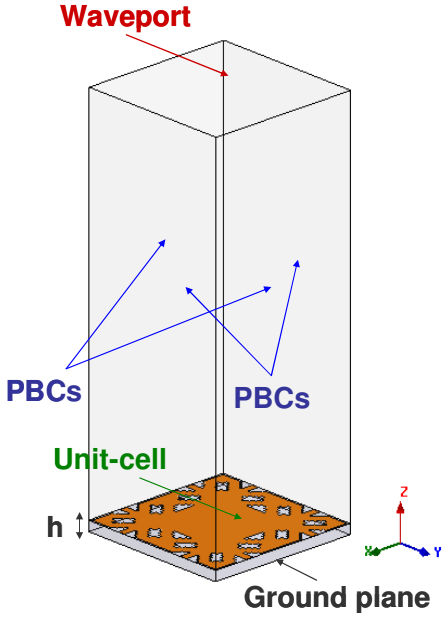

Figure 2: Simulation set-up for determining the reflection properties of the AMC.

At the resonance frequency an AMC behaves as a PMC exhibiting high surface impedance due to a very low value (ideally null) of the tangential magnetic field. To verify this fact, simulations have been carried out for a normal incident plane wave using the setup of Fig 2 (with PBCs so that the structure mimics an infinite AMC). Fig 3. shows the magnetic field variation along a plane at three different positions of the AMC unit-cell for different frequencies. As it could be expected, at the resonance frequency (6GHz) the magnetic field (H) on the periodic surface considerably decreases compared to its value at the other frequencies out of the AMC frequency band.

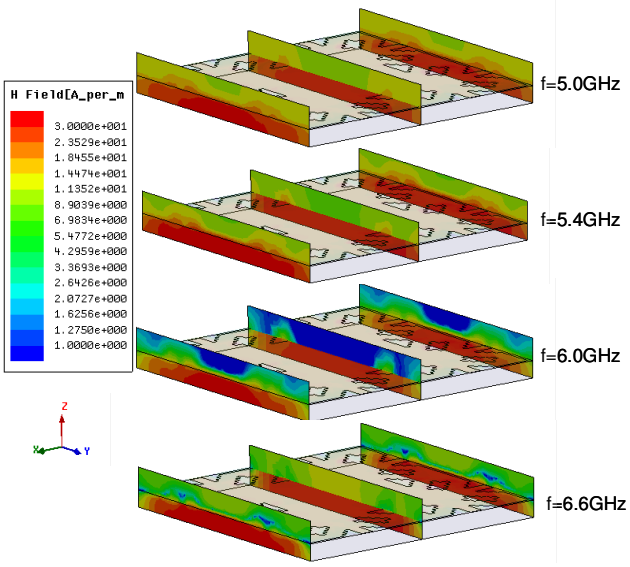

Figure 3: Magnetic field distribution on an AMC unit-cell with periodic boundary conditions at different frequencies.

Angular stability [14] is a key fact in AMC design and even more in flexible ones as in may of the intended applications, such as RFID tags or wearable antennas, it has a direct impact on their performance. For example, when combining and AMC with an antenna for an RFID tag, the AMC angular stability influences the antenna radiation performance and so the reading range. In sum, it is desirable an AMC with as higher angular stability as possible.

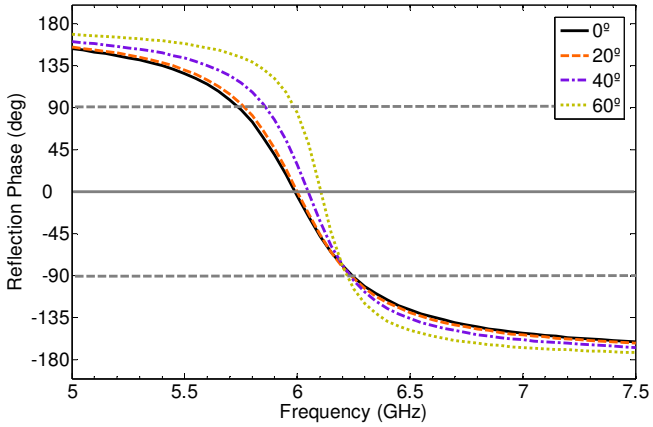

Figure 4: Simulation results of AMC reflection coefficient phase for TE polarization under different incidence angles θ_{inc}=0º, 20º, 40º and 60º .

Concerning AMC stability for different polarizations of the incident electric field, this can be ensured by using a symmetric design as the one presented in this contribution which exhibits four symmetry planes.

The reflection coefficient phase versus frequency for different incident angles θ_{inc} between 0º and 60º has been simulated for transverse electric (TE) polarized waves aiming to study the angular stability margin [14] of the presented structure. From Fig. 4 it can be obtained the absolute and relative deviations of the resonant frequency which are respectively 96MHz and 1.6%. So, it can be concluded that the presented AMC design is highly stable as it exhibits an angular margin of θ_{inc}=±60º.

3. AMC prototype characterization

A 12x12 cells AMC prototype has been manufactured using laser micromachining. The prototype physical size is 14.4cm x 14.4cm

Fig. 5 shows the reflection coefficient measurement setup in anechoic chamber (similar to the one used in [15]). Two horn antenna probes working in the band 5-7 GHz have been chosen as Tx and Rx, being 3m the separation between each probe and the object-under-test. The followed methodology [2],[15] is based on the utilization of a reference measurement (a metallic plate considered as PEC) to calculate the reflection coefficient of the AMC and is in fact the same used for the full-wave simulation. Taking into account the measured prototypes physical size (PEC and AMC have the same size), for the upper frequency (f = 7 GHz), the far field distance (RFF = $2D^2$ / λ) is $RFF_{,7GHz}$ ~ 0.97m, whereas for the lower frequency (f = 5 GHz) it decreases until $RFF_{,5GHz}$ ~ 0.69m. So the prototypes have been measured in far field conditions.

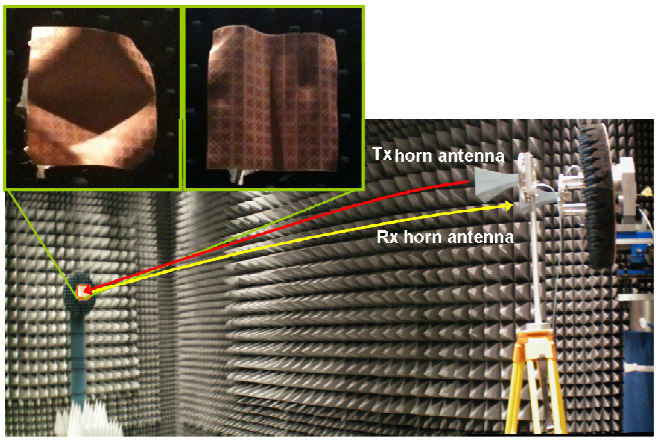

Figure 5: Reflection coefficient measurement set-up in anechoic camber.

There are many possible ways of bending an AMC. Two typical different bending patterns for the AMC have been selected and tested (see Fig.6) a "creeping" pattern which can be caused in textile AMC integrated in the garment for example when the arm is bent at the elbow, and a "smooth" pattern which can be caused in the torso or in the shoulder.

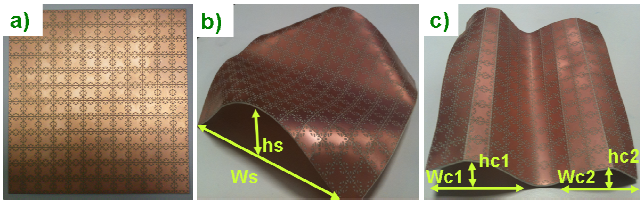

Figure 6: AMC manufactured prototype and bending patterns: a) Flat manufactured prototype b) smooth prototype with Ws=125mm, and hs=30mm; c) creeping prototype with Wc1=60mm, Wc2=52mm, hc1=18mm, and hc2=15mm

The measured reflection phase of the flat and bent manufactured prototypes for normal incidence conditions are shown in Fig. 7. The flat prototype has the resonance at 6.178GHz which means a 2.9% deviation with respect to the simulation (6.0GHz) due to under-etching in the laser micromachining. There is no frequency shift for the creeping bent prototype with respect to the flat prototype resonance, whereas the smooth bent prototype has its resonance at 6.208GHz, which means just a 1.69% deviation with respect to the flat prototype.

The flat prototype shows a 430MHz (6.96%) AMC operation bandwidth in good agreement with simulated value (8.33%) whereas the creeping bent prototype exhibits 625MHz (10.07%) and the smooth bent AMC shows 487MHz (8.02%), even slightly wider than that of the flat prototype.

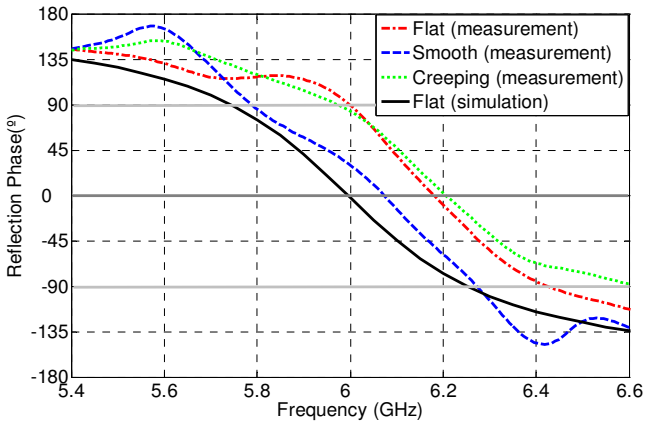

Figure 7: AMC reflection coefficient phase under flat and bent conditions.

Under normal incidence (θ_{inc} = 0º) the flat prototype presents the same reflection phase for any polarization due to the unit cell symmetry. In the case of the bent prototype, this invariance with respect to the polarization angle is also present.

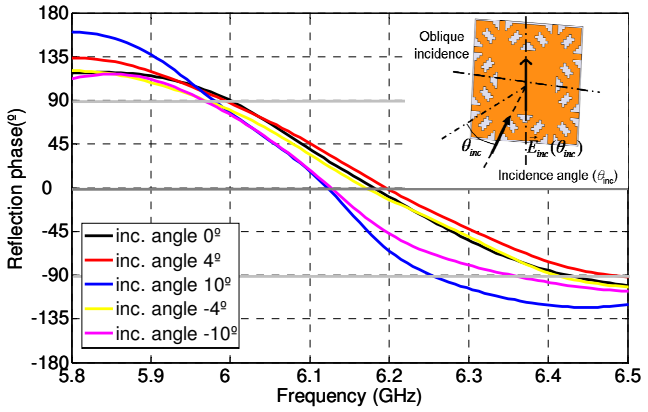

Figure 8: Reflection coefficient phase of the manufactured flat prototype for different incident angles (θ_{inc}).

The reflection coefficient phase versus frequency, for different incident angles θ_{inc} has been measured. As it was explained in the previous section, simulation results (see Fig.4) show an angular margin of θ_{inc}=±60º for transverse electric (TE) polarized waves with 1.6% relative deviation of the resonant frequency. In measurement this angular margin decreased due to finite size of prototypes. For the flat prototype resonance conditions are met within an angular margin of θ_{inc}=±10º (see Fig.8) whereas for the smooth and creeping bent prototypes (see Fig.9 and Fig.10) the obtained angular margin is θ_{inc}=±8º.

These results show that it is possible to obtain a flexible AMC without reducing the bandwidth of AMC performance with respect to a rigid AMC that uses the same unit cell design and preserving its angular stability under oblique incidence.

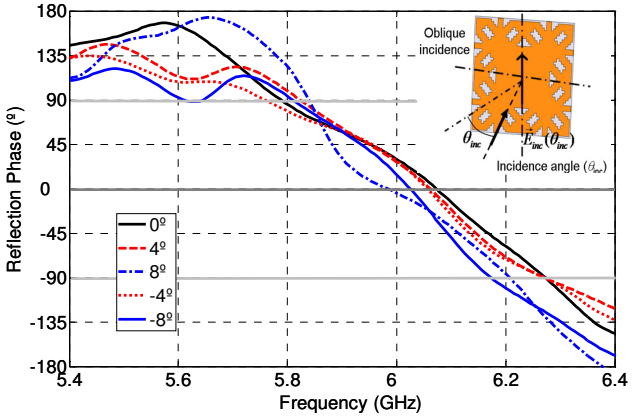

Figure 9: Reflection coefficient phase of the manufactured smooth prototype for different incident angles (θ_{inc}).

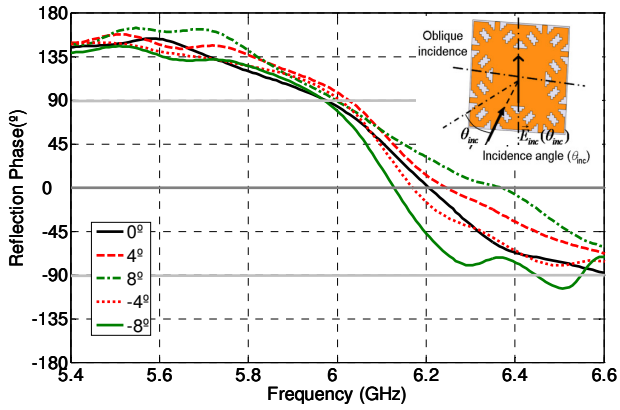

Figure 10: Reflection coefficient phase of the manufactured creeping prototype for different incident angles (θ_{inc}).

4. Conclusions

The presented novel uniplanar low-profile flexible AMC design without via holes exhibits broad AMC operation bandwidth, polarization angle independency under normal incidence and high angular stability under oblique incidence. Its low cost, simple fabrication and integration make it very attractive for applications involving antennas in RFID tags, wearable systems, and RCS reduction.

Acknowledgements

Work supported by the Ministerio de Ciencia e Innovación of Spain /FEDER under projects TEC2008-01638/TEC (INVEMTA) and CONSOLIDER-INGENIO CSD2008-00068 (TERASENSE), by the Gobierno del Principado de Asturias (PCTI)/FEDER-FSE under project PC10-06 (FLEXANT).

References

[1] G. Goussetis, A. P. Feresidis, and J.C.Vardaxoglou "Tailoring the AMC and EBG Characteristics of Periodic Metallic Arrays Printed on Grounded Dielectric Substrate", IEEE Trans. Antennas Propag., Vol.54, no.1, pp. 82-89, Jan 2006.

[2] D. Sievenpiper, L. Zhang, R. F. Jimenez Broas, N. G. Alexópolous and E. Yablonovithc, "High-impedance electromagnetic surfaces with a forbidden frequency band", IEEE Trans. Microwave Theory Tech., vol.47, no. 11, pp.2059-2074, Nov.1999

[3] F. R. Yang, K. P. Ma, Y. Qian, and T. Itoh, "A uniplanar compact photonic-bandgap (UC-PBG) structure and its applications for microwave circuit", IEEE Trans. Microwave Theory Tech., vol 47, no.8, 1509-1514, 1999

[4] D. J. Kern, D. H. Werner, A. Monorchio, L. Lanuza, and M. J. Wilhelm, "The design synthesis of multiband artificial magnetic conductors using high impedance frequency selective surfaces", IEEE Trans. on Antennas and Propag., Vol.53, No. 1, Jan. 2005.

[5] Y. Zhu, A. Bossavit and S. Zouhdi, "Surface impedance models for high impedance surfaces", Applied Physics A: Materials Science & Processing, Volume 103, Number 3, pp 677-683, 2011.

[6] M. Grelier, F. Linot, A.C. Lepage, X. Begaud, J.M. Le Mener and M. Soiron: "Analytical methods for AMC and EBG characterisations", Applied Physics A: Materials Science & Processing, Vol. 102, N.2, feb. 2011.

[7] R. C. Hadarig, M. E. de Cos, Y. Álvarez, and F. Las-Heras "Novel Bow-tie–AMC Combination for 5.8-GHz RFID Tags Usable with Metallic Objects" IEEE AWPL, Vol 9, pp 1217-1220, 2010.

[8] M. Mantash, A-C. Tarot, S. Collardey and K. Mabjoubi "Dual-band antenna for W-LAN applications with EBG", Proceedings of Metamaterials'2011, Barcelona, pp. 456 – 458, 10-15 October 2011, Spain.

[9] M. Mantash, A.C. Tarot, S. Collardey, K. Mahdjoubi, "Dual-band CPW-fed G-antenna using an EBG structure," Antennas and Propagation Conference (LAPC), Loughborough, pp. 453–456, 2010.

[10] S. Zhu and R. Langley, "Dual-Band Wearable Textile Antenna on an EBG Substrate", IEEE Trans. on Antennas and Propag., Vol.57, No. 4, April 2009.

[11] P. Salonen and Y. Rahmat-Samii, "WEBGA-wearable electromagnetic band-gap antenna", IEEE APS Int. Symp. Dig., vol.1, 451-4, Monterrey, CA, June 2004.

[12] María Elena de Cos, Yuri Álvarez, Fernando Las-Heras, "A novel approach for RCS reduction using a combination of Artificial Magnetic Conductors," Progress In Electromagnetics Research PIER 107, 147-159, 2010

[13] M. Paquay J-C. Iriarte, I. Ederra, R. Gonzalo and P. de Maagt "Thin AMC Structure for Radar Cross Section Reduction," IEEE Trans. on Antennas and Propag., vol. 55, No. 12, pp. 3630-3638, Dec 2007

[14] C. R. Simovski, P. de Maagt, S.A. Tretyakov, M. Paquay and A.A. Sochava, "Angular stabilisation of resonant frequency of artificial magnetic conductors for TE-incidence," Electron. Lett., vol. 40, no. 2, pp.92–93, Jan. 2004.

[15] M. E. de Cos, Y. Álvarez and F. Las-Heras, "Planar Artificial Magnetic Conductor: Design and Characterization setup in the RFID SHF Band", JEMWA, Vol 23, 1467-1478, 2009.

[16] A. P. Feresidis, G. Goussetis, S. Wang, and J. C. Vardaxoglou, "Artificial magnetic conductor surfaces and their application to low profile highgain planar antennas," IEEE T.A.P. vol. 53 no. 1 pp. 209–215, Jan. 2005.

[17] Ansoft HFSS, from Ansoft Corporation, Four Station Square Suite 200, Pittsburgh, PA 15219.